Glycoconj J (2012) 29:491–502
DOI 10.1007/s10719-012-9411-4

Small molecules containing hetero-bicyclic ring systems compete with UDP-Glc for binding to WaaG glycosyltransferase

Jens Landström · Karina Persson · Christoph Rademacher · Magnus Lundborg · Warren Wakarchuk · Thomas Peters · Göran Widmalm

Received: 2 February 2012 / Revised: 31 May 2012 / Accepted: 4 June 2012 / Published online: 19 June 2012

Abstract The α-1,3-glucosyltransferase WaaG is involved in the synthesis of the core region of lipopolysaccharides in *E. coli*. A fragment-based screening for inhibitors of the WaaG glycosyltrasferase donor site has been performed using NMR spectroscopy. Docking simulations were performed for three of the compounds of the fragment library that had shown binding activity towards WaaG and yielded 3D models for the respective complexes. The three ligands share a hetero-bicyclic ring system as a common structural motif and they compete with UDP-Glc for binding. Interestingly, one of the compounds promoted binding of uridine to WaaG, as seen from STD NMR titrations, suggesting a different binding mode for this ligand. We propose these compounds as scaffolds for the design of selective high-affinity inhibitors of WaaG. Binding of natural substrates, enzymatic activity and donor substrate selectivity were also investigated by NMR spectroscopy. Molecular dynamics simulations of WaaG were carried out with and without bound UDP and revealed structural changes compared to the crystal structure and also variations in flexibility for some amino acid residues between the two WaaG systems studied.

Keywords Glycosyltransferase · Inhibitor · NMR · Molecular modeling · Screening

Electronic supplementary material The online version of this article (doi:10.1007/s10719-012-9411-4) contains supplementary material, which is available to authorized users.

J. Landström · M. Lundborg · G. Widmalm (✉)
Department of Organic Chemistry, Arrhenius Laboratory,
Stockholm University,
106 91, Stockholm, Sweden
e-mail: gw@organ.su.se

K. Persson
Department of Chemistry, Umeå University,
901 87, Umeå, Sweden

C. Rademacher · T. Peters
Institute of Chemistry, University of Luebeck,
Ratzeburger Allee 160,
23538, Luebeck, Germany

W. Wakarchuk
National Research Council of Canada,
Institute for Biological Sciences,
100 Sussex Drive,
Ottawa, ON K1A 0R6, Canada

Lipopolysaccharide (LPS) [1] is a fundamental component of the gram-negative bacterial outer membrane. It constitutes a major component of the outer leaflet and plays a crucial role as a barrier and as a means of interaction with the outside environment. The LPS is divided into three parts; the hydrophobic Lipid A anchor, the core oligosaccharides (core OS) consisting of 10–15 sugars, and a structurally diverse O-antigen [2]. The core OS can be divided into two regions, the inner and the outer core. The inner core OS, which comprises L-*glycero*-D-*manno*-heptose (heptose) and 3-deoxy-D-*manno*-oct-2-ulosonic acid (Kdo), is relatively conserved as compared to the outer core that varies among different strains. The core oligosaccharides are assembled by a number of glycosyltransferases (GTs), organized in operons. The first hexose of the outer core is added by the α-1,3-glucosyltransferase WaaG by the transfer of a D-glucosyl group from UDP-Glc onto L-*glycero*-D-*manno*-heptose II. The protein sequence of WaaG is highly conserved (>85 % identity) among the different *Escherichia coli* and *Salmonella* core types [3]. WaaG belongs to the CAZy classification GT-4 family (GT4) [4] and catalyzes a retaining transferase reaction in which the α-stereochemistry of the donor glucose residue is retained in the product. The crystal structure

[5] reveals that the enzyme folds into a GT-B fold with two Rossman-like domains. The donor sugar binding site and the acceptor site (large enough to accommodate the two first heptose moieties of the inner core) are located in the cleft formed between the two domains.

While inverting glycosyl transfer reactions are assumed to follow a direct displacement mechanism, in analogy with the inverting glycosidases, the reaction catalyzed by retaining transferases has caused much more debate [6–8]. The double-displacement mechanism used by the retaining glycosidases involves the formation of a covalent glycosyl-enzyme intermediate. This is however not a likely mechanism for the retaining GTs since many of the crystal structures have revealed side chain amides, or as in WaaG, a main chain amide, close to the anomeric carbon of the donor sugar, in perfect position for a nucleophilic attack. Given that amides are unlikely candidates for nucleophilic attack reactions, a mechanism involving the formation of a short-lived ion pair intermediate has been proposed for the retaining GTs [8]. If an understanding of the molecular recognition process of WaaG can be obtained and inhibitors be developed, a new class of anti-infective/antibiotic will be available for these bacterial pathogens as well as an insight into the functions of this enzyme [9].

NMR spectroscopy offers a variety of techniques to characterize the interaction between enzymes and their ligands in solution [10]. Both quantitative [11] and qualitative [12] information of the binding event can be obtained by ligand detected techniques in solution without isotope labeling. In this study NMR spectroscopy was used to characterize the interactions between WaaG and natural substrates as well as small compounds from a fragment library [13] to identify WaaG-inhibitors. We also report an NMR-based activity assay based on the enzyme-catalyzed hydrolysis of the donor substrate UDP-Glc and investigated the selectivity of WaaG towards different donor substrates.

Conformational dynamics of proteins plays a critical role in biochemical processes and is crucial for an understanding of molecular recognition. Molecular dynamics (MD) simulations are being utilized to study dynamic phenomena on an atomic level [14]. GTs are known to be flexible enzymes [15]; we have therefore used MD simulations with explicit water to investigate the dynamic properties of WaaG upon substrate binding.

In this study we present for the first time an exhaustive study of natural donor and acceptor substrates, recognition and dynamic properties of the WaaG GT. A fragment-based screening has also been carried out and identified compounds which can be used as starting points for development of potent inhibitors.

Materials and methods

Cloning, protein expression and purification The plasmid pCW::*waaG* encoding *E. coli waaG* was used as a template to amplify the gene for subcloning into pET-M11. The gene fragment was PCR amplified using primers 5′ TTTTTCCATGGTCGTTGCTTTTTGTTTATATA3′ and 5′ AAAAAGGTACCTCAACCATCCAGACCACCCGT-3′ (restriction sites underlined). The PCR product was cleaved with *Acc65I* and *NcoI* and subcloned into the pET-M11 expression vector (EMBL, Germany). The final plasmid encodes an N-terminal His_6-tag followed by a cloning vector linker (PMSDYDIPTTENLYFQGA) and WaaG (1–374). The construct was expressed in *E. coli* BL21 (DE3) pLysS at 37 °C in LB media supplemented with 50 $\mu g \cdot mL^{-1}$ kanamycin and 25 $\mu g \cdot mL^{-1}$ chloramphenicol. When the culture reached an OD_{600} of 0.6 the temperature was lowered to 18 °C and the expression was induced with 0.5 mM IPTG. The cells were harvested by centrifugation after an additional 18 h of growth. Pellets were resuspended in lysis buffer (50 mM NaH_2PO_4 pH 8.2, 200 mM NaCl, 50 mM L-arginine, 1 % Triton X-100 and 10 mM imidazole) supplemented with EDTA-free protease inhibitor cocktail (Roche) and lyzed on ice by sonication. Cellular debris was removed by centrifugation and the supernatant was loaded onto a column packed with 3 mL Ni-NTA (Qiagen). After being washed with 100 mL wash buffer (50 mM NaH_2PO_4 pH 8.2, 200 mM NaCl and 20 mM imidazole) the protein was eluted with 10 mL elution buffer (50 mM NaH_2PO_4 pH 8.2, 200 mM NaCl and 300 mM imidazole). The protein was concentrated and the buffer was exchanged to 50 mM KH_2PO_4 pH 8.2, 200 mM NaCl, 1 mM EDTA and 0.5 mM TCEP before the protein was further purified by gel filtration on a Superdex 200 16/60 PG column (Amersham Biosciences). The purified protein was typically concentrated to 10–40 $mg \cdot mL^{-1}$ and the buffer was exchanged to 25 mM KH_2PO_4 pH 8.2, 150 mM NaCl. Aliquots of the protein (50 μL) were flash frozen in liquid N_2 and stored at −80 °C until further use.

General NMR spectroscopy The NMR experiments were carried out on a Bruker Avance III 700 MHz NMR spectrometer with a 5 mm TCI Z-gradient high resolution cryogenic probe and a Bruker Automatic Sample Changer B-ACS 60. The data from the NMR experiments were processed and analyzed with Bruker TOPSPIN 2.1 software. Two different buffers were used for the NMR studies. A 25 mM sodium phosphate buffer with different sodium chloride concentrations that was prepared in H_2O to a pH of 6.6. The H_2O-based buffer was exchanged to D_2O by lyophilization. A 60 mM potassium phosphate buffer with different sodium chloride concentrations that was prepared in H_2O to a pH of 8.2 and exchanged to D_2O as described above. The protein concentrations were measured at 280 nm using a Varian Cary 50 Bio UV–VIS spectrophotometer and a theoretical molar extinction coefficient of 41,990 $M^{-1}cm^{-1}$. All buffer exchanges were performed at 3,000 × g using an Amicon Ultra filter device

(Millipore) with a molecular weight cut-off of 10,000 Da. Uracil, uridine, UMP, UDP, UTP, UDP-Glc, α-D-Glc*p*-1-phosphate, α-D-Glc-OMe and α-D-Man-OMe were purchased from Sigma-Aldrich. UDP-Gal was a kind gift from Beat Ernst (University of Basel, Switzerland). L-*glycero*-α-D-*manno*-Hep*p*-OMe and Hep7Hep-OMe were synthesized by Garegg *et al.* [16]. For the ^{1}H NMR assignments, the proton chemical shifts and coupling constants were refined using NMR spin simulation [17] with the PERCH NMR software (PERCH Solutions Ltd., Kuopio, Finland).

Handling of the Ro3 Maybridge Library Compounds from the Ro3 Maybridge 2006 Library (Thermo Fisher Scientific Inc.) were prepared by dissolving them to a final concentration of 2 mM in 25 mM sodium phosphate buffer. Stock solutions of compounds with a lower calculated solubility were prepared at 1 mM. Compounds that showed any kind of precipitates or higher order aggregates readily visible by eye, were spun down for 20 min at 10,000 × g and the supernatant was introduced into the screening process after concentration determination by NMR using 0.4 mM sodium 3-trimethylsilyl-(2,2,3,3-$^{2}H_4$)-propanoate (TSP, δ_H 0.00) as an internal reference. Peak-picking of ^{1}H resonances in all reference spectra of the compounds enabled distribution of the compounds from the Maybridge library into 25 bins using the ^{1}H chemical shifts of the individual compounds as selection rules. The compounds were distributed such that that all compounds would have at least one unique resonance that did not overlap with any other peak, *i.e.*, a chemical shift difference of at least 0.01 ppm. The number of compounds in each bin ranged from 11 to 20 with an average of 18 compounds [18].

NMR screening All NMR screening data were measured at 282 K using Norell S-3-HT-7 3 mm tubes. Samples for STD NMR screening contained 15 μM WaaG, compounds from the library at a concentration of approximately 60 μM each and 10 μM of TSP in a 25 mM phosphate buffer containing 150 mM NaCl dissolved in D_2O. A competition experiment with UDP was performed at a concentration of UDP of 600 μM in solution. Reference bins, containing only the Maybridge compounds in D_2O phosphate buffer and TSP, were also prepared. The STD experiments were recorded using the standard pulse sequence [19] with a 15 ms 5 kHz spin-lock pulse to reduce the background protein resonances and excitation sculpting [20] with a 164 Hz square π-pulse to suppress residual HDO. Saturation of the protein ^{1}H NMR signals of the enzyme were performed using a train of 80 selective 69 Hz Gaussian pulses with duration of 50 ms, adding up to a total saturation time of 4 s. The on-resonance frequency was set to 0.4 ppm and off-resonance irradiation was applied at 80 ppm. STD NMR spectra were acquired with a total of 768 transients in addition to 16 scans to allow the sample to reach a steady state. Experiments were performed with a spectral width of 9 kHz and 20,480 data points corresponding to an acquisition time of 1.1 s and an additional relaxation delay of 0.1 s giving a total repetition time of 5.2 s. The TSP resonance was used as a reference for classifying STD effects. Four categories, 0 to 3 were used where category 0 corresponds to absence of an STD effect and category 1 corresponds to equal or lower STD effects than observed for TSP. Ligands in category 2 show larger STD effects than observed for TSP, and category 3 comprises compounds that display large STD effects (>8 %). The 58 donor site hits with an STD score of 3 (*vide infra*) were: 9, 24, 26, 29, 30, 32, 47, 65, 86, 98, 106, 115, 135, 141, 145, 148, 160, 161, 162, 170, 171, 176, 192, 193, 196, 199, 214, 219, 243, 262, 264, 266, 276, 284, 301, 307, 308, 311, 316, 346, 362, 370, 375, 379, 382, 394, 396, 398, 408, 409, 419, 438, 442, 446, 452, 483, 488, 500; the 77 non-binder compounds having score zero were: 5, 11, 12, 13, 16, 17, 20, 28, 52, 59, 62, 67, 75, 95, 128, 129, 130, 131, 156, 163, 174, 180, 201, 211, 212, 216, 221, 225, 235, 240, 247, 258, 259, 260, 285, 286, 287, 303, 305, 306, 318, 321, 322, 326, 327, 328, 335, 340, 341, 349, 351, 353, 361, 372, 373, 377, 406, 407, 413, 416, 417, 429, 430, 432, 449, 459, 461, 466, 467, 468, 476, 484, 489, 490, 494, 498, 499 [18].

Inter-Ligand Overhauser Effect (ILOE) Two different sets of compounds from the Maybridge Library were prepared for screening. Samples for the first ILOE screening contained 38 μM protein, 114 Maybridge Library compounds, having the score 3 in the STD screening, at a concentration of approximately 50 μM each, 79 μM UDP, 5 μM TSP, 88 mM phosphate buffer and 150 mM NaCl dissolved in D_2O. A reference sample without WaaG was also prepared. Samples for the second ILOE screening contained 27 μM protein, 56 Maybridge Library compounds, having the STD score 3 and not competing with UDP in the STD screening, at a concentration of approximately 80 μM each, 300 μM UDP-Glc, 5 μM TSP, 68 mM phosphate buffer and 200 mM NaCl dissolved in D_2O. A reference sample without WaaG was also prepared. The ILOE NMR experiments were carried out using the standard phase-sensitive NOESY pulse sequence (τ_{mix}=800 ms) with excitation sculpting and a 165 Hz square π-pulse, to suppress residual HDO and purge pulses to suppress unwanted magnetization. The experiment was performed with 4,096 data points in the direct dimension, 288 increments in the indirect dimension, with a spectral width of 5 kHz, in both dimensions, and a relaxation delay of 1.4 s. For each increment 112 scans were acquired and 16 scans were used to allow the sample to reach a steady state.

Uridine competition screening In total 61 compounds, 58 donor site specific binders with STD score 3 and three with

score zero (*vide supra*), were subjected to ranking with competitive STD experiments against uridine. The samples contained 0.2 mM of uridine, 1.7 μM WaaG, compounds from the library at a concentration of approximately 0.5 mM and 10 μM of TSP in 25 mM phosphate buffer containing 200 mM NaCl. The STD experiments were performed with a 15 ms 5 kHz spin-lock pulse, excitation sculpting with a 164 Hz square π-pulse, protein saturation using a train of 60 selective 68 Hz Gaussian pulses with duration of 50 ms, a saturation time of 3 s, on-resonance frequency at 0.5 ppm and off-resonance irradiation at 80 ppm. Spectra were acquired with a total of 640–1,024 transients in addition to 32 scans to allow the sample to reach a steady state, a spectral width of 9 kHz and 16 k data points corresponding to an acquisition time of 0.9 s and an additional relaxation delay of 0.1 s giving a total repetition time of 4 s for the experiment. The changes in STD effects of the uridine resonances upon compound addition were monitored and compared to a theoretical STD inhibition curve of uridine calculated as described by Dalvit *et al.* [21].

K_D measurements The dissociation constant, K_D, of uridine was measured at 293 K using transverse relaxation rates, R_2, of the protons in uridine at 8 different concentrations (0.056–4.7 mM) and a constant WaaG concentration of 5 μM. T_2 values were measured using CPMG experiments with 12 different delays ranging from 0.01 to 4 s, 24 k data points with a spectral width of 8 kHz, 40–96 scans per delay time and a relaxation delay of 10 s. The R_2 values were calculated using MATLAB (The Mathworks, Inc.), plotted against the uridine concentrations (Figure S1) and the value of K_D was extracted [11] using the curve fitting tool in MATLAB. The K_D of UDP was measured using competitive STD experiments against uridine with 8 different UDP concentrations (0.8–8,000 μM) (Figure S2) and constant uridine and WaaG concentrations of 0.8 mM and 12 μM, respectively. The K_D value of UDP was extracted [21] using the curve fitting tool in MATLAB.

STD experiments on UDP-glycosides STD experiments to detect binding of natural substrates were performed in 60 mM potassium phosphate buffer, 200 mM of sodium chloride, WaaG concentrations ranging from 0.05 to 0.15 mM and ligand concentrations ranging from 0.5 to 5 mM. The STD experiments were performed with a 15 ms 5 kHz spin-lock pulse, excitation sculpting with a square π-pulse (150–200 Hz), protein saturation using a train of 80 selective 55–70 Hz Gaussian pulses with duration of 50 ms, saturation times between 0.5 and 4 s, on-resonance frequencies of −1, 0.5, 0.9 and 7 ppm, and off-resonance irradiation at 60 ppm. Spectra were acquired with a total of 256–2,048 transients in addition to 32 scans to allow the sample to reach a steady state, a spectral width of 9 kHz and 16 k data points corresponding to an acquisition time of 0.9 s.

Hydrolysis of UDP-glycosides To investigate the hydrolytic activity of WaaG, samples with 300 μM of UDP-Glc or UDP-Gal and 0.6 μM of WaaG were dissolved in 60 mM potassium phosphate buffer with 150 mM sodium chloride and 10 μM TSP. Reference samples without WaaG were also prepared. The samples were kept at room temperature. ^{1}H experiments with a presaturation rf strength of 16 Hz to suppress residual HDO were collected with 128 transients a couple of days apart up to 70 days.

Molecular mechanics The simulations used NAMD [22, 23] (parallel version, 2.6) employing a CHARMM22 force field with CMAP [24]. Initial coordinates of WaaG were taken from the crystal structure 2IW1 that also contains uridine-5′-diphospho-2-deoxy-2-fluoro-α-D-glucose [5]. The protein structure was solvated using TIP3P water molecules and counter ions generated in VMD [25]. Subsequent energy minimization was carried out with UDP in the donor site. The resulting WaaG structure was used without water molecules for molecular docking and with water molecules for MD simulations.

Molecular docking Four programs were utilized for docking, *viz*., Glide, Autodock, Autodock Vina and SurflexDock. The programs employ different docking and scoring algorithms, meaning that the generated poses as well as the ranking of them are expected to be different. In all cases the protein structure used was the energy minimized conformation mentioned above with UDP removed. In the first case docking was performed using Glide (Glide, version 5.0, Schrödinger, LLC, New York, NY, 2008) in the Maestro suite (Maestro, version 8.5, Schrödinger, LLC, New York, NY, 2008). The dimensions of the grid box were 25 Å in all dimensions and the ligand midpoint box was 14 Å in all dimensions. In order to make the grid box encompass the binding site without making it too large uridine-5′-diphospho-2-deoxy-2-fluoro-α-D-glucose, from 2IW1, was used as a guide. The uridine part of it was superimposed on uridine in the protein structure from molecular mechanics and the center of the grid box was positioned at the anomeric carbon. The van der Waals radii scaling factor was kept at unity for receptor atoms with a partial charge lower than 0.25. The ligands docked were number 32, 214 and 370 from the Maybridge library as well as uridine and uridine-5′-diphosphate. The docking was performed using extra precision (XP) and 20 poses were saved per ligand. The other parameters were used as default. Docking was carried out on a PC using an Intel(R) Pentium(R) 4 CPU 3.40 GHz processor with 2 GB RAM running the Ubuntu 9.04 operating system.

The second program used for docking was Autodock 4.00 [26]. Starting from the same protein structure as described above partial charges [27] were added using AutoDock Tools [28]. The grid box was generated with 60×60×

60 points at a 0.375 Å resolution, equaling 22.5 Å in all directions. The grid center was at approximately the same position as the center of the Glide grid box. The five ligands were prepared in AutoDock Tools by adding partial charges [29] and specifying rotatable bonds, without applying any restrictions to them. The docking was performed with 65,000 generations, 300 local iterations, 100 runs, a population size 20 and a mutation rate of 0.15. The small population size and high mutation rate were based on the findings of Haupt [30]. The number of evaluations used in the docking procedure depended on the number of rotatable bonds in the ligands. For compounds from the Maybridge Library 7,500,000 evaluations were used for ligands 32, 214 and 370 while uridine and UDP used 22,500,000 and 37,500,000, respectively. The other parameters were used as default. The docking was performed on an Intel(R) Core (TM) 2 Quad CPU Q6600 2.40 GHz processor with 4 GB RAM running Ubuntu 9.04 64 bit operating system.

The third program employed in docking was Autodock Vina version 1.0.2 [31]. The same files for proteins and ligands that were used for Autodock were also used for docking with Autodock Vina. The docking procedure used the same coordinates for the center of the grid as for Autodock, but the dimensions were 30 Å in x, y and z dimensions. The exhaustiveness of the docking was increased from 8 to 16 and 25 binding modes were generated. The dockings were performed on an Intel(R) Core(TM) 2 Quad CPU Q6600 2.40 GHz processor with 4 GB RAM running Ubuntu 9.04 64 bit operating system.

The fourth program used for docking was Surflex-Dock version 2.415 [32]. To create the protomol (the idealized pseudo-molecular target used by Surflex-Dock for docking the ligands) UDP and the energy minimized protein were saved separately. The protomol was created using the ligand as a guide. The protomol volume was expanded by 6 Å (proto_bloat 6). The docking was performed using the same ligands as in the other dockings and with the -pgeomx flag to use the more exhaustive docking accuracy parameter set, including pre- and post-docking energy minimization, using 6 starting conformations of each ligand, requiring poses to have RMS differences of at least 0.5 Å to be considered unique and increasing the number of retained poses to 20. The dockings were run on an Intel(R) Pentium(R) 4 CPU 3.40 GHz processor with 2 GB RAM running the Ubuntu 9.04 operating system.

Molecular dynamics (MD) simulations The MD simulation [22–24] of WaaG with UDP present was started from the solvated energy minimized structure (*vide supra*). The *apo*-form of the structure was generated by removing UDP from the model. The MD simulations were carried out with multiple-time-stepping and 2 fs, 2 fs, and 6 fs were used as the inner, middle and outer time steps in the NPT ensemble (P=1 atm, 293 K) with a cutoff distance for non-bond interactions set at 12 Å and periodic boundary conditions giving box sizes of approximately 71×70×65 Å. The smooth particle-mesh Ewald (SPME) method was used to calculate the full electrostatic interactions. The temperature and pressure were kept constant using a Langevin thermostat and a Langevin barostat, respectively. All bonds to hydrogen atoms were kept rigid. Subsequent to energy minimization, heating and 1 ns of equilibration, production runs of WaaG in the *apo*-form and in complex with UDP were carried out for 55 ns each. Data were saved every 2,500 time steps for analysis. Trajectory analyses, alignments and plotting were carried out with VMD and MATLAB. Pictures of molecular models were rendered using the Pymol software. Mean value filtering of the three-dimensional surface was performed with a 11×11 square kernel using an in-house MATLAB script.

Results

NMR spectroscopy The proton NMR chemical shifts and coupling constants of donors and related compounds were assigned (Table S1) by standard NMR spectroscopy experiments and refined by NMR spin simulation using the PERCH NMR software. STD NMR experiments were performed on these compounds (Fig. 1) in the presence of WaaG to determine binding epitopes. UDP-Glc, UDP-Gal, UTP, UDP, UMP and uridine gave large STD effects whereas for α-D-Glc*p*-1-phosphate, uracil and α-D-Glc-OMe they were very low or absent.

WaaG carries out the transfer of a glucosyl group to a heptose residue in the LPS synthesis. Therefore, as models for the acceptor substrate α-D-Man-OMe, L-*glycero*-α-D-*manno*-Hep*p*-OMe and Hep7Hep-OMe (Fig. 1) were tested for binding. The STD experiments did not show any effects for these compounds suggesting either low or no affinity.

Dissociation constants, K_Ds, were measured for uridine and UDP. For uridine the K_D was obtained by fitting R_2 relaxation rates measured by ^{1}H CPMG experiments at different concentrations of uridine, using a constant WaaG concentration [11, 33]. UDP affinity was subsequently deduced by competitive STD NMR experiments against uridine [19]. The resulting K_Ds at 293 K were 0.6 mM and 9 μM for uridine and UDP, respectively. These affinities are in same range as K_Ds reported for other GTs [34]. It may be noted that in cases when the binding is very tight and as a result the off rates are quite low the transfer of saturation to the ligand in solution will not be very efficient [10].

GT activity and selectivity of WaaG in the absence of a natural acceptor substrate were investigated by studying if WaaG was able to hydrolyze the natural substrate UDP-Glc.

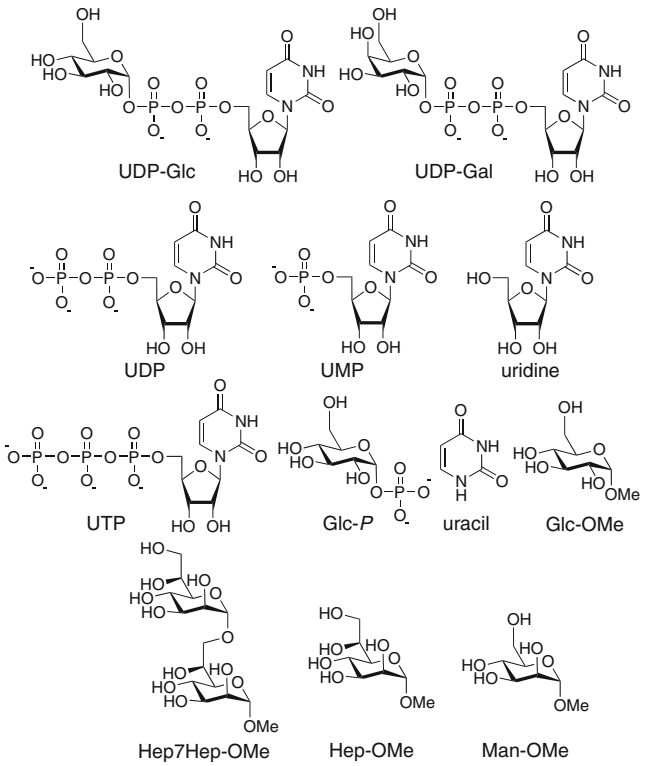

Fig. 1 Donor substrate, related compounds and potential acceptor compounds that have been tested for binding using NMR spectroscopy

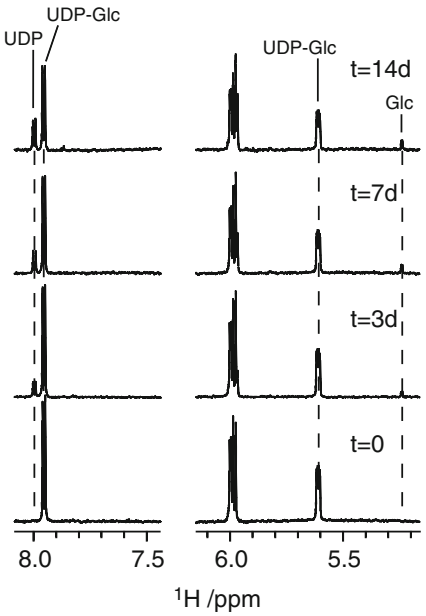

Fig. 2 ^{1}H NMR spectra of the time dependency of hydrolysis of UDP-Glc (0.3 mM) in the presence of WaaG (0.6 μM)

The GT-catalyzed hydrolysis of the donor substrate should differ from the hydroxyl ion dependent hydrolysis of nucleotide sugars. A WaaG catalyzed hydrolysis of UDP-Glc, would yield Glc and UDP, but hydrolysis of UDP-Glc in buffer without WaaG would give a 1,2-cyclic phosphate of Glc and UMP [34, 35]. UDP-Glc and UDP-Gal were each dissolved in buffer together with WaaG at room temperature and ^{1}H NMR spectra were collected to monitor the reactions (Fig. 2). Reference samples without WaaG were also prepared and evaluated. Slow GT-catalyzed hydrolysis was observed of UDP-Glc in presence of WaaG, but hydrolysis of UDP-Gal or any of the reference samples was not detected. When UDP-glycosyl samples (without enzyme) were left for several weeks we could observe hydrolysis as well as decomposition. However, since WaaG GT is only stable for a couple of days in solution at ambient temperature UDP-Glc was not completely hydrolyzed.

The Maybridge fragment library, which contains 500 compounds of M_ws from 94 to 291 Da, was used in the search of compounds with affinity for WaaG. The use of fragment-based libraries is advantages compared to high-throughput screening with drug-sized molecules since the hit-rate is higher and the fragments possess high ligand efficiency, *i.e.*, binding affinity per heavy atom. Furthermore, <1,000 compounds need to be screened [36] thereby making the selected Maybridge fragment library a good choice. ^{1}H NMR spectra were recorded for all the compounds and solubility was checked (*vide supra*). The compounds were then distributed into 25 bins [18] *via* an algorithm that was designed to minimize spectral overlap of resonance signals (0.01 ppm cutoff value) and that there was at least one unique proton chemical shift for each compound [37]. STD NMR experiments were carried out on WaaG and all the bins having a subset of compounds from the library. In order to identify compounds with binding affinity for the donor site of WaaG, a competition experiment with UDP was performed (Fig. 3). The compounds were ranked from 0 to 3 according to STD intensities relative the internal reference TSP. The results of the screening of 448 compounds from the Maybridge library against WaaG are summarized in Table 1.

In order to rank the hits from the STD experiments, competitive screening versus uridine was performed on 61 compounds (58 specific donor site hits with STD score 3 and three compounds having score zero). Uridine in the presence of WaaG gives large STD effects (Fig. 4), making the experiments very sensitive. The changes in STD effects of the uridine signals were monitored upon addition of compounds from the Maybridge library. From the competitive screening three compounds were selected (Fig. 5). Compounds 32 and 370 gave reduction of the STD effect for uridine of approximately 30 %, giving estimated K_Ds between 0.5 and 1 mM for the two compounds when compared to a theoretical inhibition curve of uridine [21]. Compound 214 gave a 70 % enhancement of the STD effect for uridine. Notably, the compound showed competition against UDP in the first screening round. The other compounds did not give reductions or enhancements of the uridine STD

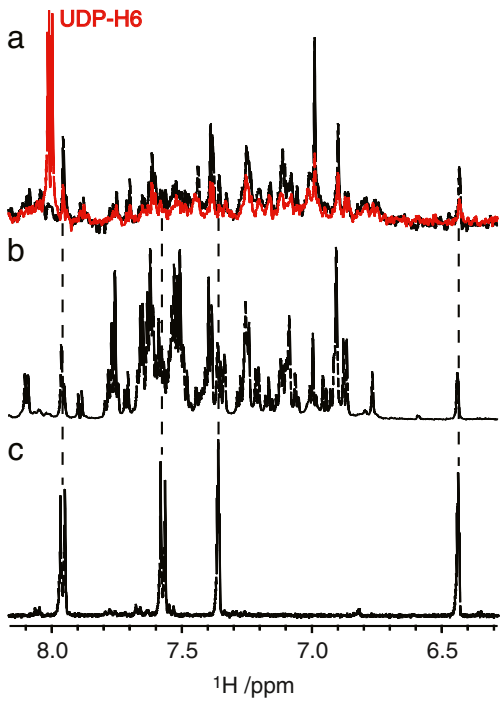

Fig. 3 **a** STD NMR spectra of WaaG and screening of compounds in bin 2, containing 20 compounds, with UDP in red and without UDP in black (on-resonance irradiation at 0.4 ppm for 3.0 s); **b** ^{1}H NMR reference spectrum of WaaG and compounds in bin 2; **c** ^{1}H NMR spectrum of compound 214

effects of more than 15 %, which was considered to be within the estimated error for the measurements. The compounds identified by NMR screening were subsequently investigated using molecular modeling techniques. In addition, ^{1}H,^{1}H-NOESY experiments were performed on WaaG and 114 Maybridge Library compounds that had an STD ranking of 3 to investigate the presence of ILOEs [38, 39]. The experiments were carried out in two sets with either UDP or UDP-Glc present. However, the ^{1}H,^{1}H-NOESY experiments did not reveal any ILOEs. Different mixing times were also used but in the present experimental setup the limiting parameter was most probably the low ligand-to-

Table 1 WaaG screening statistics showing the number of fragment hits and the STD ranking. The pie diagram to the right shows the fractions of donor- and non-donor site binders with an STD score >1, compared to the non-binders

STD score	Donor site	Non-donor site	Total
0	0	74	74
1	18	109	127
2	36	96	132
3	58	57	115
Total	112	336	448

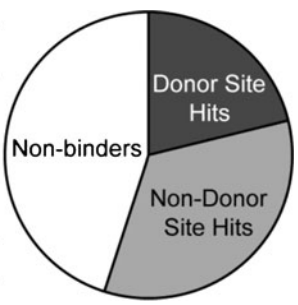

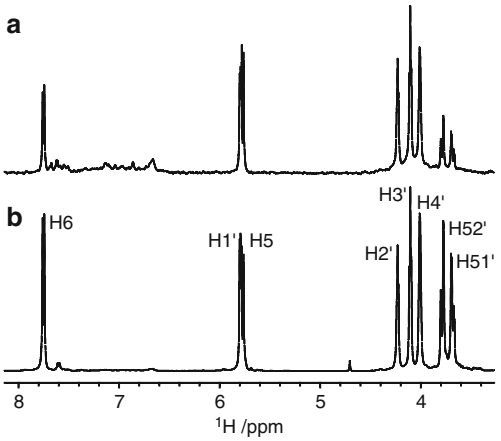

Fig. 4 **a** STD NMR spectrum of uridine (2.6 mM) and WaaG (8 μM) scaled 16 times; **b** ^{1}H NMR reference spectrum of uridine. Protons in the sugar are denoted by a prime and in the base they are non-primed

protein ratio, which in other studies has been reported [38, 39] to be an order of magnitude higher than those used herein. It cannot be completely ruled out that ILOEs may be observed at much higher ligand to protein ratios. As ILOE screening has not been in the focus of the present study that aims at identification of binding fragments to WaaG we have not made any further attempts at this time to identify potential ILOEs.

Molecular docking The three compounds selected from the competitive screening against uridine were docked into the energy minimized structure of WaaG, using Glide, Autodock, Autodock Vina and Surflex-Dock softwares. The RMSD of the protein backbone atoms between the crystal structure and the structure used in docking was 0.91 Å. The results from all four docking programs yielded similar docking poses for each of the compounds (Fig. 6), but ranked in different order. For the docking simulations experimental restraints were taken into account in the sense that uridine, UDP, 32 and 370 are expected to bind to the same site, while 214 competes with UDP and promotes binding of uridine and thus binds to a different subsite of the UDP-Glc binding pocket.

The top ranked poses of the Glide docking agreed well with experimental data in that UDP, 32 and 370 occupied the same part of the binding site. Compound 214 was docked overlapping with UDP, but not with uridine. The carboxyl group of 214 interacted with Lys209, in the same

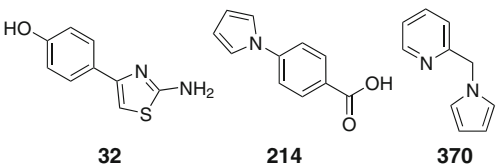

Fig. 5 Structures of the two compounds, 32 and 370, which compete best with uridine, and compound 214

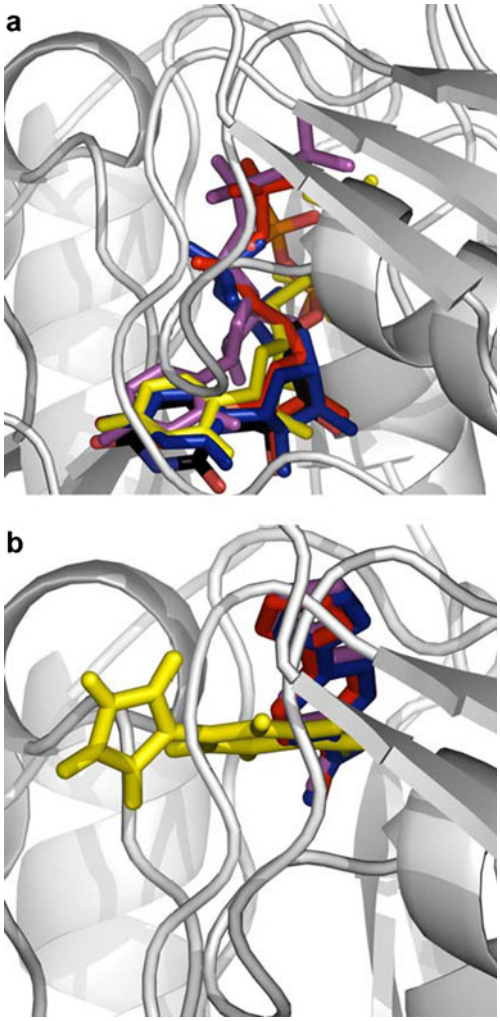

Fig. 6 Superimposed docking poses, from Glide (*red*), Autodock (*blue*), Autodock Vina (magenta) and Surflex (*yellow*), of **a** UDP and **b** 214. The crystal structure of UDP from the WaaG-UDP complex (2IW1) is shown in **a** colored by atom type

region as the diphosphate group of UDP. The RMSD of the top ranked pose of UDP, compared to the crystal structure (2IW1), was as high, 6.6 Å, with good agreement only for the uridine group. Uridine had an RMSD of 3.0 Å compared to uridine in the protein structure from molecular mechanics. The complexes of WaaG and ligands are depicted in Fig. 7.

With Autodock, the binding mode proposed with Glide of 370 had the second best estimated binding free energy, but showed the largest cluster. The expected pose of 214, based on experimental data, was ranked fourth according to the estimated free energy of binding from Autodock. The top ranked poses of UDP, uridine and 32 agreed well with the Glide results. The RMSD of the top ranked UDP pose, compared to the crystal structure, was 4.5 Å, with the phosphate tail at a different angle. Uridine had an RMSD of 3.8 Å.

Autodock Vina found the expected pose of compound 214 at position 7 out of 25. The UDP pose that most closely resembled the crystal structure 2IW1 was ranked at position 10 and had an RMSD of 5.1 Å, with deviations both in the uridine and diphosphate groups, while the RMSD of uridine was 3.6 Å. The top poses of the other docked ligands were in agreement with the experimental data in that they were placed in the uridine binding site.

The Surflex-Dock results differed more from the Glide dockings and the anticipated poses based on experimental data. The RMSDs of UDP and uridine were 5.2 and 3.2 Å, respectively. The higher RMSD of UDP was caused mainly by the diphosphate side chain. The top ranked poses of 32 were placed where 214 was expected to bind and pose 10 of 32 was arranged such that it could replace uridine. The dockings of 214 did not agree well with the results from the other programs, but the 3rd pose in its result list would still replace UDP, but not uridine; thus, not conflicting with experimental data. The two top poses of 370 were placed where 214 would be expected to bind, but the third pose was docked as anticipated.

It is difficult to fairly evaluate the docking results since only UDP has been crystallized in complex with WaaG, while uridine had the advantage of being included in the energy minimization of the protein prior to docking. All programs generated good poses of these two ligands except for Autodock Vina that did not rank the expected UDP pose very well. In general the RMSDs of UDP and uridine are quite high, presumably caused by the protein input structure employed in the docking. It is clear that these docking programs generate comparable poses of the docked ligands, but they are ranked differently. This illustrates the problem of scoring and ranking results from docking [40, 41]. In this study a consensus between experimental data and results from docking has been used to suggest plausible binding modes, but with higher quality scoring methods docking results could be more confidently relied upon.

Molecular dynamics simulations Two 55 ns MD simulations, with explicit water as solvent, were carried out on WaaG and in complex with UDP. The crystal structure of WaaG, 2IW1 [5], was used as the starting point for the molecular model. In the analysis the data was mean value filtered by replacing each point value with the mean value of its surroundings [42]. This has the effect of eliminating points that are unrepresentative of their surrounding environments in order to observe only larger structural changes. During the first half of the simulation of the *apo*-form of WaaG (0–28 ns), limited flexibility was present (Fig. 8), where only three amino acids had backbone RMSDs >2.0 Å, *viz*., Lys47 with 2.21 Å, Phe113 with 2.27 Å, and Tyr115 with 2.45 Å. After approximately 28 ns, a structural transition in the protein occurred. In this latter structure (Fig. 9), four amino acids had backbone RMSDs ≥2.0 Å, *viz*., His59 with 2.60 Å, Phe113 with 2.26 Å, Leu114 with 2.00 Å, and Ala283 with 2.29 Å, during the remaining period of the simulation (28–55 ns). The average backbone RMSD over all

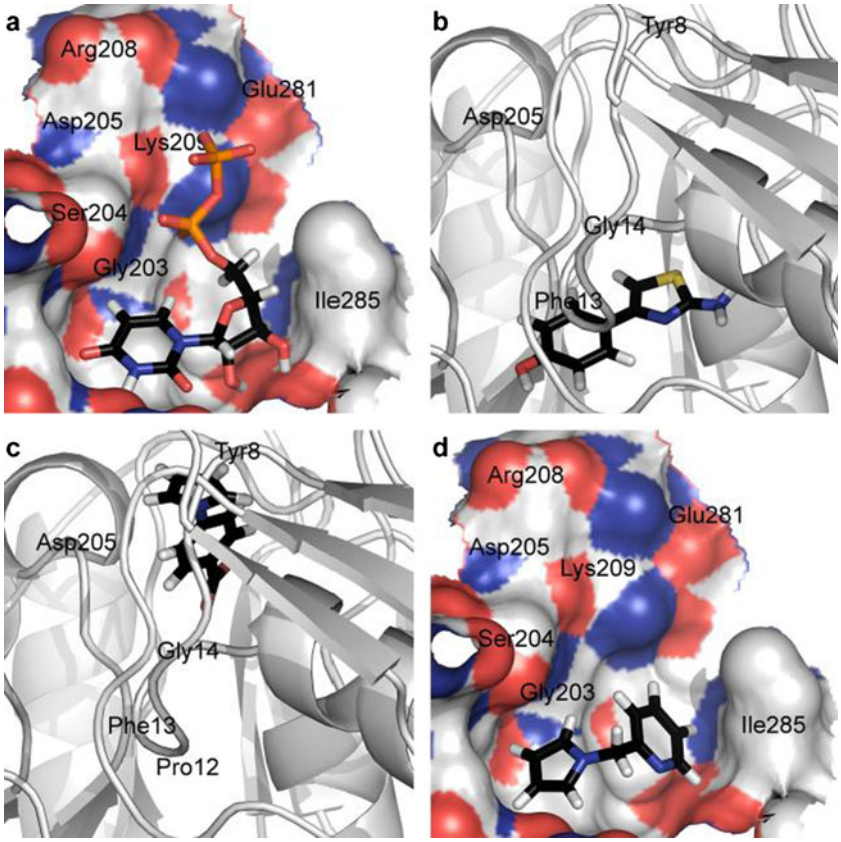

Fig. 7 Proposed binding of **a** UDP, **b** 32, **c** 214 and **d** 370, in complex with WaaG from docking simulations using Glide. All pictures show the same region of the enzyme

residues is similar between the two structures being 0.97 Å during 0–28 ns and 0.96 Å during 28–55 ns. For the WaaG-UDP complex a structural transition also occurs (Fig. 8), but at a later point in the MD simulation, *i.e.*, at about 48 ns. During the 0–48 ns period (Fig. 9), larger backbone RMSDs of >2.5 Å are observed for His59 with 2.59 Å, Phe113 with 2.53 Å, Glu194 with 2.53 Å, Arg240 with 3.01 Å, Leu357 with 3.61 Å, and Tyr358 with 3.91 Å. In the structure complex after the transition the largest backbone RMSDs >2.0 Å were observed for Lys47 with 2.23 Å, Phe113 with 2.44 Å, and Arg240 with 2.23 Å. The WaaG-UDP complex had the average backbone RMSD over all residues larger for the former structure being 1.16 Å during 0–48 ns and smaller for the latter structure being 0.92 Å during 48–55 ns.

The flexibility of Lys47, situated far from the binding site in a small loop, was similar for all four structures and did not change to a large extent depending on the presence or absence of the bound UDP ligand. Likewise, the region where Phe113, Leu114, and Tyr115 reside, closer to the binding site, shows higher flexibility in both the *apo*-form and the complexed form of WaaG. For the WaaG-UDP complex Arg240 is quite flexible, being part of an α-helix. In the binding region the flexibility is low with an RMSD of 0.70 Å for Ala283 in the UDP complex after the structural transition took place. In addition, the backbone RMSDs for Leu357 and Tyr358 are low in the second part of the WaaG-UDP simulation, *viz.*, 1.16 Å and 0.94 Å, respectively.

Discussion

The results from the NMR-based interaction studies with the donor substrate antagonists suggest that the binding of the donor substrate is determined by the nucleoside part and not by the carbohydrate part, a finding that has also been observed in earlier studies on other GTs [43], consistent with the fact that both UDP-Glc and UDP-Gal have similar affinities towards WaaG according to the STD experiments. The binding of the acceptor is probably very weak and not easily detectable by STD NMR experiments. The weak affinity for the acceptor substrate is reflected by reported K_M values in the mM range for some GTs [44].

We have shown that the study of the hydrolysis of the donor substrate by GTs is a convenient way to obtain information on selectivity and activity of the enzyme, because often the donor of a GT is known, but in many cases the acceptor is unknown or very difficult to access. The results show that WaaG is selective towards UDP-Glc, compared to UDP-Gal, in the glycosylation although it has a similar affinity to both the compounds. The approach can also be used as a tool in screening for inhibitors where the glucose production can be monitored.

By using results from NMR screening and docking, the agonist 214 can be linked with either of the other two compounds, 32 and 370, and probably a potent inhibitor can be obtained. The results also show the strength of a

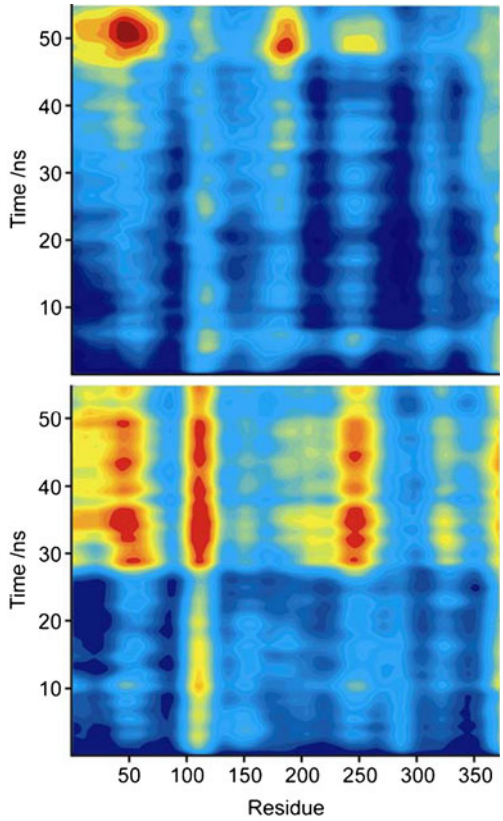

Fig. 8 Mean value filtered time- and residue dependency of the backbone RMSD of WaaG from the 55 ns MD simulations relative to crystal structure 2IW1. The UDP-complex and *apo*-form of WaaG are shown in the top and bottom panels, respectively. Blue color indicates low RMSD and red color high RMSD

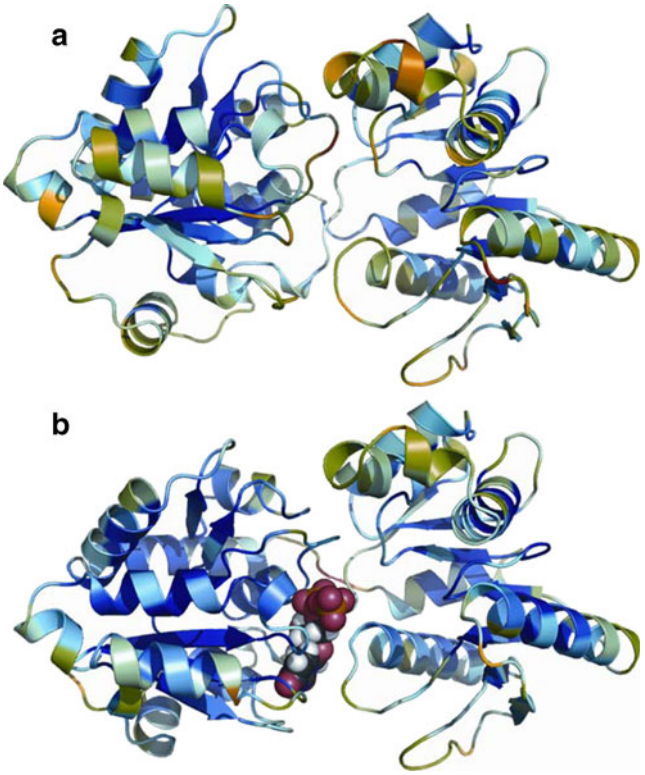

Fig. 9 WaaG colored by RMSD of the backbone relative to its average structure during a part of the MD simulation where red color indicates a high RMSD and blue a low RMSD; **a** *Apo*-form of WaaG during 28–55 ns and **b** WaaG in complex with UDP (space-filling model in standard color coding) during 0–48 ns

competitive screening approach; thus, agonists can be found that are not easily picked up by other screening setups. The threshold for detecting the weakly binding compounds of the fragment library is mainly determined by the affinity of the reporter ligand. If a ligand with lower affinity to WaaG than uridine would have been available, more low affinity inhibitors could have been retrieved. The fragment-based screening shows that many compounds are binding to other sites than the donor site of WaaG. A reason for this can be that several hydrophobic pockets are present on the surface of WaaG and can indicate that the enzyme is to some extent associated with a membrane in the cell. We also note that high hit rates have been reported for fragment-based screenings of other GTs [18]. The three compounds 32, 214 and 370 from the Maybridge fragment library shown to bind to WaaG in this study were not found among the best ten binders to human blood group B galactosyltransferase [18] nor in the screening for inhibitors to norovirus [37]. The structural differences in WaaG, from the MD simulations, between the *apo*-form (28–55 ns) and the UDP-complexed form (0–48 ns) presented in Fig. 9 may be described by a hinge-based motion where the two protein domains rotate relative to each other as a result of binding UDP. Conformational changes between 'open and closed' forms of GTs have been reported *e.g.* for glycogen synthases where the domain-domain closure was evident [45], being 15° in one of the cases [46]. For the PimA mannosyltransferase, which has structural similarities to WaaG [47], significant conformational changes and interdomain rearrangements take place upon binding of GDP-Man [48]. Very large alterations in the 3D-structure occurred for the MshA GT upon binding of the donor sugar with a 97° rotational reorientation of the N- vs. C-domain [49]. The nature of the conformational changes in WaaG upon binding of the donor sugar UDP-Glc may thus consist of closure and rotational movements between the two domains, but the extent to which these movements occur is still an open question.

In conclusion, the fragment-based library screening of WaaG used NMR spectroscopy methods to find, out of 500, in particular three compounds that were bound in the active site of the GT. Molecular docking techniques were utilized to find structural poses of the ligands making use of the recently reported crystal structure. Two of the compounds were proposed to bind similar to uridine whereas the third compound is positioned in the region of WaaG where the glucosyl residue of UDP-2-deoxy-2-fluoro-α-D-Glc*p* in the crystal binds. Thus, making scaffolds for inhibitor design based on linking one of the former molecular

fragments with the latter may result in high affinity inhibitors. A conformational change, upon substrate binding, has been reported for a GT with a different fold [15], and may be important for WaaG having a GT-B fold, but the precise nature of such a change requires further investigations.

Acknowledgments This work was supported by grants from the Swedish Research Council, The Knut and Alice Wallenberg Foundation, The Åke Wiberg Foundation, Fonds der Chemischen Industrie, and Deutscher Akademischer Austausch Dienst. We thank Gunter Stier, EMBL, Germany for cloning vectors.

References

1. Raetz, C.R.H., Whitfield, C.: Lipopolysaccharide endotoxins. Annu. Rev. Biochem. **71**, 635–700 (2002)
2. Amor, K., Heinrichs, D.E., Frirdich, E., Ziebell, K., Johnson, R.P., Whitfield, C.: Distribution of core oligosaccharide types in lipopolysaccharides from *Escherichia coli*. Infect. Immun. **68**, 1116–1124 (2000)
3. Heinrichs, D.E., Yethon, J.A., Whitfield, C.: Molecular basis for structural diversity in the core regions of the lipopolysaccharides of *Escherichia coli* and *Salmonella enterica*. Mol. Microbiol. **30**, 221–232 (1998)
4. Cantarel, B.L., Coutinho, P.M., Rancurel, C., Bernard, T., Lombard, V., Henrissat, B.: The Carbohydrate-Active enZymes database (CAZy): an expert resource for glycogenomics. Nucleic Acids Res. **37**, D233–D238 (2009)
5. Martinez-Fleites, C., Proctor, M., Roberts, S., Bolam, D.N., Gilbert, H.J., Davies, G.J.: Insights into the synthesis of lipopolysaccharide and antibiotics through the structures of two retaining glycosyltransferases from family GT4. Chem. Biol. **13**, 1143–1152 (2006)
6. Davies, G.J., Gloster, T.M., Henrissat, B.: Recent structural insights into the expanding world of carbohydrate-active enzymes. Curr. Opin. Struct. Biol. **15**, 637–645 (2005)
7. Breton, C., Šnajdrová, L., Jeanneau, C., Koča, J., Imberty, A.: Structures and mechanisms of glycosyltransferases. Glycobiology **16**, 29R–37R (2006)
8. Lairson, L.L., Henrissat, B., Davies, G.J., Withers, S.G.: Glycosyltransferases: structures, functions, and mechanisms. Annu. Rev. Biochem. **77**, 521–555 (2008)
9. Yethon, J.A., Vinogradov, E., Perry, M.B., Whitfield, C.: Mutation of the lipopolysaccharide core glycosyltransferase encoded by *waaG* destabilizes the outer membrane of *Escherichia coli* by interfering with core phosphorylation. J. Bacteriol. **182**, 5620–5623 (2000)
10. Meyer, B., Peters, T.: NMR spectroscopy techniques for screening and identifying ligand binding to protein receptors. Angew. Chem. Int. Ed. **42**, 864–890 (2003)
11. Fielding, L.: NMR methods for the determination of protein-ligand dissociation constants. Prog. Nucl. Magn. Reson. Spectrosc. **51**, 219–242 (2007)
12. Mayer, M., Meyer, B.: Group epitope mapping by saturation transfer difference NMR to identify segments of a ligand in direct contact with a protein receptor. J. Am. Chem. Soc. **123**, 6108–6117 (2001)
13. Fischer, M., Hubbard, R.E.: Fragment-based ligand discovery. Mol. Interv. **9**, 22–30 (2009)
14. Adcock, S.A., McCammon, J.A.: Molecular dynamics: survey of methods for simulating the activity of proteins. Chem. Rev. **106**, 1589–1615 (2006)
15. Milac, A.L., Buchete, N.V., Fritz, T.A., Hummer, G., Tabak, L.A.: Substrate-induced conformational changes and dynamics of UDP-*N*-acetylgalactosamine:polypeptide *N*-acetylgalactosaminyltransferase-2. J. Mol. Biol. **373**, 439–451 (2007)
16. Garegg, P.J., Oscarson, S., Szönyi, M.: Synthesis of methyl 3-O-(α-D-glucopyranosyl)-7-O-(L-*glycero*-α-D-*manno*-heptopyranosyl)-L-*glycero*-α-D-*manno*-heptopyranoside. Carbohydr. Res. **205**, 125–132 (1990)
17. Laatikainen, R., Niemitz, M., Weber, U., Sundelin, J., Hassinen, T., Vepsäläinen, J.: General strategies for total-lineshape-type spectral analysis of NMR spectra using integral-transform iterator. J. Magn. Reson. **120**, 1–10 (1996)
18. Rademacher, C., Landström, J., Sindhuwinata, N., Palcic, M.M., Widmalm, G., Peters, T.: NMR-based exploration of the acceptor binding site of human blood group B galactosyltransferase with molecular fragments. Glycoconjugate J. **27**, 349–358 (2010)
19. Mayer, M., Meyer, B.: Characterization of ligand binding by saturation transfer difference NMR spectroscopy. Angew. Chem. Int. Ed. **38**, 1784–1788 (1999)
20. Hwang, T.-L., Shaka, A.J.: Water suppression that works. Excitation sculpting using arbitrary wave-forms and pulsed-field gradients. J. Magn. Reson. **112**, 275–279 (1995)
21. Dalvit, C., Fasolini, M., Flocco, M., Knapp, S., Pevarello, P., Veronesi, M.: NMR-based screening with competition water-ligand observed via gradient spectroscopy experiments: detection of high-affinity ligands. J. Med. Chem. **45**, 2610–2614 (2002)
22. Kalé, L., Skeel, R., Bhandarkar, M., Brunner, R., Gursoy, A., Krawetz, N., Phillips, J., Shinozaki, A., Varadarajan, K., Schulten, K.: NAMD2: greater scalability for parallel molecular dynamics. J. Comput. Phys. **151**, 283–312 (1999)
23. Phillips, J.C., Braun, R., Wang, W., Gumbart, J., Tajkhorshid, E., Villa, E., Chipot, C., Skeel, R.D., Kalé, L., Schulten, K.: Scalable molecular dynamics with NAMD. J. Comput. Chem. **26**, 1781–1802 (2005)
24. Mackerell Jr., A.D., Feig, M., Brooks III, C.L.: Extending the treatment of backbone energetics in protein force fields: limitations of gas-phase quantum mechanics in reproducing protein conformational distributions in molecular dynamics simulations. J. Comput. Chem. **25**, 1400–1415 (2004)
25. Humphrey, W., Dalke, A., Schulten, K.: VMD: visual molecular dynamics. J. Mol. Graph. **14**, 33–38 (1996)
26. Morris, G.M., Goodsell, D.S., Halliday, R.S., Huey, R., Hart, W.E., Belew, R.K., Olson, A.J.: Automated docking using a Lamarckian genetic algorithm and an empirical binding free energy function. J. Comput. Chem. **19**, 1639–1662 (1998)
27. Weiner, S.J., Kollman, P.A., Case, D.A., Singh, U.C., Ghio, C., Alagona, G., Profeta Jr., S., Weiner, P.: A new force field for molecular mechanical simulation of nucleic acids and proteins. J. Am. Chem. Soc. **106**, 765–784 (1984)
28. Sanner, M.F.: Python: a programming language for software integration and development. J. Mol. Graphics Mod. **17**, 57–61 (1999)
29. Gasteiger, J., Marsili, M.: A new model for calculating atomic charges in molecules. Tetrahedron Lett. **34**, 3181–3184 (1978)
30. Haupt, R.L.: Optimum population size and mutation rate for a simple real genetic algorithm that optimizes array factors. Antennas and Propagation Society International Symposium, IEEE **2**, 1034–1037 (2000)
31. Trott, O., Olson, A.J.: AutoDock Vina: improving the speed and accuracy of docking with a new scoring function, efficient optimization, and multithreading. J. Comput. Chem. **31**, 455–461 (2010)
32. Jain, A.N.: Surflex: fully automatic flexible molecular docking using a molecular similarity-based search engine. J. Med. Chem. **46**, 499–511 (2003)
33. Verdier, L., Gharbi-Benarous, J., Bertho, G., Evrard-Todeschi, N., Mauvais, P., Girault, J.-P.: Dissociation-equilibrium constant and bound conformation for weak antibiotic binding interaction with

different bacterial ribosomes. J. Chem. Soc. Perkin Trans. 2. 2363–2371 (2000). doi:10.1039/B007666J
34. Sindhuwinata, N., Munoz, E., Javier Munoz, F., Palcic, M.M., Peters, H., Peters, T.: Binding of an acceptor substrate analog enhances the enzymatic activity of blood group B galactosyltransferase. Glycobiology **20**, 718–723 (2010)
35. Nunez, H.A., Barker, R.: The metal ion catalyzed decomposition of nucleoside diphosphate sugars. Biochemistry **15**, 3843–3847 (1976)
36. Carr, R.A.E., Congreve, M., Murray, C.W., Rees, D.C.: Fragment-based lead discovery: leads by design. Drug Discov Today **10**, 987–992 (2005)
37. Rademacher, C., Guiard, J., Kitov, P.I., Fiege, B., Dalton, K.P., Parra, F., Bundle, D.R., Peters, T.: Targeting norovirus infection – multivalent entry inhibitor design based on NMR experiments. Chem. Eur. J. **17**, 7442–7453 (2011)
38. Li, D., DeRose, E.F., London, R.E.: The inter-ligand Overhauser effect: a powerful new NMR approach for mapping structural relationships of macromolecular ligands. J. Biomol. NMR **15**, 71–76 (1999)
39. Becattini, B., Pellecchia, M.: SAR by ILOEs: an NMR-based approach to reverse chemical genetics. Chem. Eur. J. **12**, 2658–2662 (2006)
40. Halperin, I., Ma, B., Wolfson, H., Nussinov, R.: Principles of docking: an overview of search algorithms and a guide to scoring functions. Proteins **47**, 409–443 (2002)
41. Li, X., Li, Y., Cheng, T., Liu, Z., Wang, R.: Evaluation of the performance of four molecular docking programs on a diverse set of protein-ligand complexes. J. Comput. Chem. **31**, 2109–2125 (2010)
42. Boyle, R.D., Thomas, R.C.: Computer vision: a first course. Blackwell Scientific Publications, Oxford (1988)
43. Blume, A., Angulo, J., Biet, T., Peters, H., Benie, A.J., Palcic, M., Peters, T.: Fragment-based screening of the donor substrate specificity of human blood group B galactosyltransferase using saturation transfer difference NMR. J. Biol. Chem. **281**, 32728–32740 (2006)
44. Wlasichuk, K.B., Kashem, M.A., Nikrad, P.V., Bird, P., Jiang, C., Venot, A.P.: Determination of the specificities of rat liver Gal(β1-4)GlcNAcα2,6-sialyltransferase and Gal(β1-3/4)GlcNAcα2,3-sialyltransferase using synthetic modified acceptors. J. Biol. Chem. **268**, 13971–13977 (1993)
45. Buschiazzo, A., Ugalde, J.E., Guerin, M.E., Shepard, W., Ugalde, R.A., Alzari, P.M.: Crystal structure of glycogen synthase: homologous enzymes catalyze glycogen synthesis and degradation. EMBO J. **23**, 3196–3205 (2004)
46. Sheng, F., Jia, X., Yep, A., Preiss, J., Geiger, J.H.: The crystal structures of the open and catalytically competent closed conformation of *Escherichia coli* glycogen synthase. J. Biol. Chem. **284**, 17796–17807 (2009)
47. Guerin, M.E., Kordulakova, J., Schaeffer, F., Svetlikova, Z., Buschiazzo, A., Giganti, D., Gicquel, B., Mikusova, K., Jackson, M., Alzari, P.M.: Molecular recognition and interfacial catalysis by the essential phosphatidylinositol mannosyltransferase PimA from Mycobacteria. J. Biol. Chem. **282**, 20705–20714 (2007)
48. Guerin, M.E., Schaeffer, F., Chaffotte, A., Gest, P., Giganti, D., Korduláková, J., van der Woerd, M., Jackson, M., Alzari, P.M.: Substrate-induced conformational changes in the essential peripheral membrane-associated mannosyltransferase PimA from Mycobacteria. J. Biol. Chem. **284**, 21613–21625 (2009)
49. Vetting, M.W., Frantom, P.A., Blanchard, J.S.: Structural and enzymatic analysis of MshA from *Corynebacterium glutamicum*. J. Biol. Chem. **283**, 15834–15844 (2008)